arXiv:1108.3453v1 [cond-mat.quant-gas] 17 Aug 2011

p-wave stabilization of three-dimensional Bose-Fermi solitons

N G Parker
*School of Mathematics and Statistics, Newcastle University, Newcastle Upon Tyne, UK**

D A Smith
Vienna Center for Quantum Science and Technology, Atominstitut, TU Wien, Vienna, Austria

(Dated: August 18, 2011)

We explore bright soliton solutions of ultracold Bose-Fermi gases, showing that the presence of p-wave interactions can remove the usual collapse instability and support stable soliton solutions that are global energy minima. A variational model that incorporates the relevant s- and p-wave interactions in the system is established analytically and solved numerically to probe the dependencies of the solitons on key experimental parameters. Under attractive s-wave interactions, bright solitons exist only as meta-stable states susceptible to collapse. Remarkably, the presence of repulsive p-wave interactions alleviates this collapse instability. This dramatically widens the range of experimentally-achievable soliton solutions and indicates greatly enhanced robustness. While we focus specifically on the boson-fermion pairing of ^{87}Rb and ^{40}K, the stabilization inferred by repulsive p-wave interactions should apply to the wider remit of ultracold Bose-Fermi mixtures.

PACS numbers: 03.75.Lm, 67.85.Pq

I. INTRODUCTION

The study of wave mechanics and propagation in non-linear media is a fundamental concept within physics. In particular, solitons are a general non-dispersive solution to the one-dimensional non-linear wave equation. Bright solitons have been observed in many areas of physics, such as in water [1], liquid hydrogen [2], optics [3] and atomic Bose-Einstein condensates (BECs) [4–6]. In the latter case, these self-trapped matter waves are supported by a balance between attractive atomic scattering interactions and repulsive zero-point kinetic energy between bosons. As well as being of fundamental interest in many-body quantum physics, bright matter-wave solitons are being touted for potential uses in atom interferometry [4, 5, 7, 8] and surface characterization [9]. However, when realized in three-dimensions these solitons exist only as meta-stable states prone to catastrophic collapse [10, 11].

Ultracold Bose-Fermi (BF) gases have received a great deal of recent experimental attention and have been realised through ^{7}Li-^{6}Li [12], ^{23}Na-^{6}Li [13], ^{87}Rb-^{40}K [14], ^{174}Yb-^{173}Yb [16] and ^{84}Sr-^{87}Sr [17] mixtures. At such low temperatures, the scattering of atoms with non-zero relative angular momentum is heavily restricted such that p-wave and higher interactions are typically negligible. Furthermore, the Pauli exclusion principle forbids identical fermions from interacting via s-wave collisions. Thus, for an ultracold Bose-Fermi mixture (in which the fermions are identical), the dominant interactions are s-wave boson-boson and boson-fermion interactions. It has been shown theoretically that a repulsive Bose gas and a non-interacting Fermi gas co-existing in a radial waveguide can be coupled together by an attractive boson-fermion interaction to form a self-trapped state [18, 19]. It is these 'Bose-Fermi' solitons that we will consider in this paper. We note that the ^{87}Rb-^{40}K system appears particularly well-suited to support BF solitons since its natural boson-fermion interaction is strongly attractive. However, just as in the case of an attractively-interacting 3D Bose-Einstein condensate [10, 11, 20], a 3D Bose-Fermi system is prone to collapse when the interspecies interaction becomes too attractive [15, 22–24]. While certain effects have been highlighted to raise the threshold for collapse, e.g. finite temperature effects in Bose-Fermi mixtures [25] and Feshbach resonance management [26], possession of angular momentum [27] and fragmentation [28] in Bose-Einstein condensates, the instability to collapse ultimately remains in the system.

By exploiting scattering resonances, the p-wave interaction between fermions can now be experimentally engineered to significant values [29]. It is thus the rationale of this work to explore the way in which p-wave interactions may modify Bose-Fermi soliton solutions. Our framework to perform this is a variational approach using a gaussian ansatz for the boson and fermion density distributions. Via the Gross-Pitaveskii model for the bosons and the Thomas-Fermi approximation for the fermions, we derive an analytic form for the energy of this coupled system up to p-wave interactions (for the boson-fermion and fermion-fermion interaction) and from this we obtain the variational soliton solutions. First we review the properties of the soliton solutions in the absence of p-wave interactions, in agreement with previous studies [18, 19], before considering the modifications in the presence of p-wave interactions. Specifically we focus our results on a ^{87}Rb-^{40}K mixture, due to the naturally large and attractive s-wave scattering length between the species [14, 15, 31], and fermion-fermion p-wave interactions, due to their capacity to be engineered experimen-

*Electronic address: nick.parker@ncl.ac.uk

tally [29].

II. VARIATIONAL MODEL OF BOSE-FERMI SOLITONS

A. System overview and the variational ansatz

We consider a degenerate gas of identical fermions coexisting with a Bose-Einstein condensate of bosons, all at zero temperature. Neglecting quantum and thermal fluctuations, we will model the fermion and boson gases within the mean-field picture. Each gas is confined by an axially-homogeneous waveguide potential $V_{\mathrm{B\{F\}}}(\mathbf{r}) = \frac{1}{2}m_{\mathrm{B\{F\}}}\omega^2_{\mathrm{B\{F\}}}r^2$, where $\omega_{\mathrm{B\{F\}}}$ is the radial trap frequency experienced by the bosons {fermions} and $m_{\mathrm{B\{F\}}}$ is the boson {fermion} mass. Due to the low energy of the atomic collisions, the s-wave and p-wave interactions are modelled by contact interactions characterised by a single length scale, the scattering length. Within the Bose gas, the atoms interact predominantly via s-wave scattering with characteristic length a_{B} (p-wave interactions are negligible). Within the Fermi gas, s-wave interactions are suppressed via the Pauli exclusion principle and the leading atomic interaction is p-wave with a scattering length a_{F} [23]. For overlapping clouds, the bosons and fermions additionally interact with each other, predominantly via the s-wave interaction, of lengthscale $a_{\mathrm{BF}s}$, but we will also include the corresponding p-wave interaction, with effective scattering length $a_{\mathrm{BF}p}$ [23].

Bright solitons require an attractive interaction to enable self-trapping of the wave. Here we shall consider the case where this interaction arises from the s-wave boson-fermion coupling. A rudimentary requirement is thus that the boson and fermion gases are overlapping in space and this enables us to assume the same ansatz for the boson and fermion density distributions. We will assume that the radial profile of the fermion and boson gases is a gaussian. This is an exact result in the quasi-1D limit (formally expressed as $\hbar\omega_{\mathrm{B}} \gg \mu_{\mathrm{B}}$ and $\hbar\omega_{\mathrm{F}} \gg \mu_{\mathrm{F}}$, where μ_{B} and μ_{F} are the chemical potentials of the boson gas and fermion gas, respectively [32]) for which the radial profile coincides with the gaussian ground harmonic oscillator state. In the following, we do not impose a fixed size to our gaussian profile but simply require the transverse profile to approximate a gaussian shape. Thus our approach can apply to systems that lie outside of this dimensionality condition. However, as is shown later, the radial sizes of the solitons remain close to the radial harmonic oscillator length l_{ho} throughout.

The most obvious choice for a suitable axial profile is, by analogy to 1D bright bosonic soliton result, a sech-profile [21]. However, with this choice we are unable to obtain analytic solutions for the variational energies. Karpiuk *et al.* [18] pursued this choice numerically. Instead, to obtain an analytic form for the variational energies, we employ a gaussian axial profile. From studies of bright BEC solitons it has been shown, firstly, that sech and gaussian axial profiles give very similar results, and secondly, that both forms of ansatz give very good agreement with more precise theoretical treatments, e.g. numerical solutions of the Gross-Pitaevskii equation [10, 11]. We will thus consider the boson {fermion} density $n_{\mathrm{B\{F\}}}$ to have a cylindrically-symmetric gaussian profile,

$$n_{\mathrm{B\{F\}}}(\mathbf{r}) = \frac{N_{\mathrm{B\{F\}}}}{\pi^{3/2}L_zL_r^2}\exp\left(-\frac{z^2}{L_z^2}\right)\exp\left(-\frac{r^2}{L_r^2}\right), \quad (1)$$

where L_r and L_z are the radial and axial sizes, respectively, and $N_{\mathrm{B\{F\}}}$ is the numbers of bosons {fermions}. We consider that L_r and L_z are common for both the bosons and the fermions.

Note that the validity of the mean-field Gross-Pitaevskii model for the boson gas requires that $N_{\mathrm{B}} \gg 1$. Furthermore, our description of the Fermi gas component is based on the Thomas-Fermi approximation which is valid for $N_{\mathrm{F}}^{1/3} \gg 1$ [21]. Hence our approach is strictly valid only in the regime of large N and we will only consider parameters that satisfy this.

B. Energetics of the system

We will consider the total energy density of the Bose-Fermi state $\varepsilon[n_{\mathrm{B}}, n_{\mathrm{F}}]$ to be the sum of the boson contribution $\varepsilon_{\mathrm{B}}[n_{\mathrm{B}}]$, fermion contribution $\varepsilon_{\mathrm{F}}[n_{\mathrm{F}}]$ and boson-fermion term $\varepsilon_{\mathrm{BF}}[n_{\mathrm{B}}, n_{\mathrm{F}}]$ [23]. We will proceed by modelling each energy contribution of the gaussian wavepackets in turn. Note that the energy is the volume integral of the corresponding energy density $E = \int \varepsilon[n]dV$. For a different choice of ansatz and in the absence of p-wave interactions, Karpiuk *et al.* [18] followed a similar variational approach to explore Bose-Fermi soliton solutions.

1. *Bosonic energy contribution*

The energy density of the zero-temperature boson gas, interacting via s-wave interactions of scattering length a_{B}, is provided by the Gross-Pitaevksii model [21],

$$\varepsilon_{\mathrm{B}}[n_{\mathrm{B}}] = \frac{\hbar^2}{2m}|\nabla\sqrt{n_{\mathrm{B}}}|^2 + V_{\mathrm{B}}(\mathbf{r})n_{\mathrm{B}} + \frac{2\pi\hbar^2 a_{\mathrm{B}}}{m_{\mathrm{B}}}n_{\mathrm{B}}^2. \quad (2)$$

The terms of the right-hand side represent, respectively, the kinetic, potential and interaction energies of the boson gas. For convenience we will express length in terms of the boson harmonic oscillator length $l_{\mathrm{ho}} = \sqrt{\hbar/m_{\mathrm{B}}\omega_B}$ and adopt dimensionless variational lengthscales $l_z = L_z/l_{\mathrm{ho}}$ and $l_r = L_r/l_{\mathrm{ho}}$. Furthermore, we rescale energy by the bosonic harmonic oscillator energy $\hbar\omega_{\mathrm{B}}$ via $E \to E/(\hbar\omega_{\mathrm{B}})$. Substituting $n_{\mathrm{B}}(\mathbf{r})$ into Eq. (2) and integrating over space, one arrives at the well-known expression for the total boson energy [21],

$$\frac{E_{\mathrm{B}}}{N_{\mathrm{B}}} = \frac{1}{2}\left(\frac{1}{l_r^2} + \frac{1}{2l_z^2}\right) + \frac{1}{2}l_r^2 + \frac{1}{\sqrt{2\pi}}\frac{a_{\mathrm{B}}}{l_{\mathrm{ho}}}\frac{N_{\mathrm{B}}}{l_z l_r^2}. \quad (3)$$

From this the presence of the collapse instability for attractively interacting BECs ($a_B < 0$) is clear: the interaction term (negative) dominates over all other (positive) energy contributions as the size of the wavepacket tends towards zero. While meta-stable states can be formed for certain parameters, the lowest energy state described by this equation is always a collapsed state of zero width.

2. Fermionic energy contribution

Determination of the mean-field fermionic energy density in general requires solving $N_{\rm F}$ coupled Hartree-Fock equations. In this manner, Karpiuk *et al.* [18] successfully modelled BF soliton solutions, but the approach is only tractable for of the order of 10 fermions. Instead, we will adopt an analytic form for the fermion energy density derived by Roth and Feldmeier [23]. Employing the Thomas-Fermi approximation, this approach follows from deriving the energy density of a homogeneous fermionic system and replacing the fixed density with $n_{\rm F}(\mathbf{r})$ (thus neglecting the contribution to the energy from density gradients). The Thomas-Fermi approximation is valid for the equlibrium state of a fermi gas when the fermion wavelength is much smaller than the system size. For a trapped fermi gas, it can be shown that this is satisfied when $N_{\rm F}^{1/3} \gg 1$ [21]. In agreement with this, the Thomas-Fermi approximation has been shown to give an excellent mean-field description of BF mixtures (in close agreement with Hartree-Fock calculations) for $N_{\rm F} \sim 1000$ [23, 33]. Via this approach, the energy density of the fermions (potential, kinetic and p-wave interaction terms, respectively) is [23],

$$\varepsilon_{\rm F}[n_{\rm F}] = V_{\rm F}(\mathbf{r})n_{\rm F} + \frac{3\hbar^2(6\pi^2)^{2/3}}{10m_{\rm F}} n_{\rm F}^{5/3} + \frac{(6\pi^2)^{5/3}}{5\pi m_{\rm F}}\hbar^2 a_{\rm F}^3 n_{\rm F}^{8/3}, \tag{4}$$

where $a_{\rm F}$ is the p-wave contact interaction between fermions [23]. Inserting the gaussian profile $n_{\rm F}(\mathbf{r})$ and integrating gives the total fermionic energy,

$$\begin{aligned}\frac{E_{\rm F}}{N_{\rm F}} &= \alpha\frac{m_{\rm B}}{m_{\rm F}}\left(\frac{N_{\rm F}}{l_z l_r^2}\right)^{2/3} + \frac{1}{2}\frac{m_{\rm F}}{m_{\rm B}}\left(\frac{\omega_{\rm F}}{\omega_{\rm B}}\right)^2 l_r^2 \\ &+ 4\beta\frac{m_{\rm B}}{m_{\rm F}}\left(\frac{a_{\rm F}}{l_{\rm ho}}\right)^3\left(\frac{N_{\rm F}}{l_z l_r^2}\right)^{5/3}\end{aligned} \tag{5}$$

where $\alpha = (9/50)6^{2/3}(3/5)^{1/2}\pi^{1/3} \approx 0.6743$ and $\beta = (3/160\pi^4)(3\pi/8)^{1/2}(6\pi^2)^{5/3} \approx 0.1880$.

3. Bose-Fermi energy contribution

Again under the Thomas-Fermi approximation, the interaction energy density between the bosons and fermions $\varepsilon_{\rm BF}[n_{\rm B}, n_{\rm F}]$ is [23],

$$\varepsilon_{\rm BF}[n_{\rm B}, n_{\rm F}] = \frac{2\pi\hbar^2 a_{{\rm BF}s}}{\mu} n_{\rm B} n_{\rm F} + \frac{(6\pi^2)^{5/3}}{20\pi\mu}\hbar^2 a_{{\rm BF}p}^3 n_{\rm B} n_{\rm F}^{5/3}, \tag{6}$$

where $a_{{\rm BF}s}$ is the s-wave boson-fermion scattering coefficient, $a_{{\rm BF}p}$ is the p-wave scattering length and $\mu = m_{\rm B}m_{\rm F}/(m_{\rm B}+m_{\rm F})$. For the density profiles (1) the boson-fermion interaction energy is,

$$\frac{E_{\rm BF}}{N_{\rm B}} = \frac{1}{\sqrt{2\pi}}\frac{a_{{\rm BF}s}}{l_{\rm ho}}\frac{m_{\rm B}}{\mu}\frac{N_{\rm F}}{l_z l_r^2} + \beta\frac{m_{\rm B}}{\mu}\left(\frac{a_{{\rm BF}p}}{l_{\rm ho}}\right)^3\left(\frac{N_{\rm F}}{l_z l_r^2}\right)^{5/3}. \tag{7}$$

C. Energy landscapes and obtaining the variational solutions

The total energy of our gaussian Bose-Fermi wavepackets is given by $E = E_{\rm B} + E_{\rm F} + E_{\rm BF}$. Upon fixing the experimental parameters (atom masses, atom numbers, scattering lengths and trap frequencies), the energy becomes confined to being a function of only the wavepacket size parameters l_r and l_z. This function $E(l_r, l_z)$ can be visualised as an energy landscape in which the presence of an energy minimum represents a variational solution. In practice, we numerically define this energy landscape and perform a simple computational search for such energy minima. Note that an unphysical solution can occur at the origin representing the effect of collapse. It is unphysical in the sense that a real Bose-Fermi system cannot shrink to zero size; in reality, a collapse will eventually become halted by the surge of three-body losses as the gas densities rise. At most, only one physical solution is ever present in these energy landscapes. We denote the coordinates of such a variational solution by the coordinates l_z^0 and l_r^0.

Where we map out regions of soliton solutions within a particular parameter space, e.g., $a_{{\rm BF}s} - N_{\rm F}$ space, this is done by randomly sampling combinations of these parameters. We typically restrict our numerical search to landscapes of extent $[0, 2]\ l_r \times [0, 10]\ l_z$.

We have verified that our methodology gives very close agreement with the variational stability diagram presented in Fig. 7 of [18]. Our results deviate by less than 10%, a deviation which is to be expected given the different ansatz employed.

D. Analytical limit: no p-wave interactions and $N_{\rm B} \gg N_{\rm F}$

We can gain a simplified analytic form for the total variational energy if we neglect p-wave interactions ($a_{\rm F} = a_{{\rm BF}p} = 0$) and assume $N_{\rm B} \gg N_{\rm F}$. The latter condition renders the fermion-fermion energy terms negligible and makes significant only terms involving $N_{\rm B}$. The total variational energy then reduces to,

$$\frac{E}{N_{\rm B}} = \frac{1}{2l_r^2} + \frac{1}{4l_z^2} + \frac{l_r^2}{2} + \left(N_{\rm B}\frac{a_{\rm B}}{l_{\rm ho}} + \frac{a_{{\rm BF}s}}{l_{\rm ho}}\frac{m_{\rm B}}{\mu}N_{\rm F}\right)\frac{1}{\sqrt{2\pi}l_z l_r^2}. \tag{8}$$

This form will enable us to gain physical intuition of the system and provide simple criteria for the existence of stable Bose-Fermi solitons. Importantly, it has the same form as the gaussian variational energy of a purely bosonic gas [10], but with an effective s-wave scattering length given by [24],

$$a_{\rm eff} = a_{\rm B} + a_{{\rm BF}s}\frac{N_{\rm F}}{N_{\rm B}}\left(\frac{m_{\rm F}+m_{\rm B}}{m_{\rm F}}\right). \quad (9)$$

A rudimentary requirement for the ability to self-trap is that the net interactions are attractive ($a_{\rm eff} < 0$). This places a lower bound on the ratio $N_{\rm F}/N_{\rm B}$ for which Bose-Fermi solitons can be self-supported,

$$\frac{N_{\rm F}}{N_{\rm B}} > -\frac{a_{\rm B}}{a_{{\rm BF}s}}\left(\frac{m_{\rm F}}{m_{\rm F}+m_{\rm B}}\right). \quad (10)$$

Furthermore, bright bosonic solitons are established to collapse when the scattering length is less than the critical value $a_{\rm B}^c = k_c l_{\rm ho}/N_{\rm B}$. For a 3D gaussian wavepacket the dimensionless coefficient has been shown to be $k_c = -0.778$ [10] (for other shapes of wavepacket the value differs but remains of the order of unity). This leads to an upper bound for the ratio $N_{\rm F}/N_{\rm B}$ in order to prevent collapse of the system,

$$\frac{N_{\rm F}}{N_{\rm B}} < \frac{k_c l_{\rm ho}}{N_{\rm B}a_{{\rm BF}s}}\left(\frac{m_{\rm F}}{m_{\rm F}+m_{\rm B}}\right) - \frac{a_{\rm B}}{a_{{\rm BF}s}}\left(\frac{m_{\rm F}}{m_{\rm F}+m_{\rm B}}\right). \quad (11)$$

From Eqs. (10,11) it is evident that the soliton solutions exist within a "window" of fermion atom number $N_{\rm F}$ whose width is,

$$\Delta N_{\rm F} = \frac{k_c l_{\rm ho}}{a_{{\rm BF}s}}\left(\frac{m_{\rm F}}{m_{\rm F}+m_{\rm B}}\right). \quad (12)$$

Equations (10), (11) and (12) provide us with an estimate for the locality and range over which BF solitons solutions may exist. Equation (12) indicates that the width of the soliton bands can be extended by employing weaker radial trapping and weaker Bose-Fermi scattering length. However, we will find that the soliton bands are even more restricted if the condition $N_{\rm B}/N_{\rm F} \gg 1$ is removed. Indeed, the above equations predict the existence of soliton solutions at the native Bose-Fermi scattering length $a_{{\rm BF}s} = -215a_0$. However, as we shall see, the full variational results predict that the soliton bands become vanishing narrow at this scattering length.

III. RESULTS

While our analytical results presented so far are applicable to any Bose-Fermi species, we will focus our ensuing results on a ^{87}Rb and ^{40}K mixture due to its naturally strong and attractive Bose-Fermi coupling and its prominent experimental occurence to date [14, 15]. We will assume that the atoms are spin-polarized and confined (in the radial direction) by a magnetic trap such that the trap frequencies are related via $\omega_{\rm F}/\omega_{\rm B} = (m_{\rm B}/m_{\rm F})^{1/2}$. Throughout our results we fix the boson-boson s-wave scattering length to be the experimentally measured value of $a_{\rm B} = 99a_0$ [34], where $a_0 = 5.3\times10^{-11}$m is the Bohr radius. We will consider the radial trap frequency, boson and fermion atom numbers, and remaining scattering lengths to be variables. Note that scattering lengths can typically be experimentally varied over many orders of magnitude by using magnetic and optical fields to access inter-atomic scattering resonances. In the cases where we fix the boson-fermion s-wave scattering length, we take it to be its native value of $a_{{\rm BF}s} = -215a_0$, as measured by Ferlaino *et al.* [31].

First we will explore the soliton solutions in the absence of p-wave interactions. Following this we will consider how p-wave interactions between fermions modify the soliton solutions. We will not explicitly present results for finite boson-fermion p-wave interactions but will comment on how they affect the system in Section IV.

A. Absence of p-wave interactions

1. *Soliton bands in $N_{\rm F} - a_{{\rm BF}s}$ space*

Figure 1(a) presents the soliton solutions in the parameter space of $a_{{\rm BF}s} - N_{\rm F}$ for 10^5 bosons and various radial trap frequencies [$\omega_{\rm B}/2\pi = 10$ (green solid region), 100 (blue dotted region) and 1000 Hz (black dashed region)]. For each trap frequency, the soliton solutions exist in a narrow band in the $a_{{\rm BF}s} < 0$ half-plane. (Note that on the scale of the figure these bands appear as lines). Above each band, the system is unstable to dispersion and below the band it is unstable to collapse. Each band scales approximately as $-1/N_{\rm F}$, as indicated by rearranging Eqs. (10) and (11). The bands are weakly dependent on trap frequency. Indeed their differences are only apparent on a much more magnified scale (inset of Fig.1(a)). As $\omega_{\rm B}$ is increased, the bands shift upwards in $a_{{\rm BF}s}$ and become slightly narrower. The latter change is in qualitative agreement with equations (10-12) which predict the band width to scale in proportion to $l_{\rm ho} = \sqrt{\hbar/m\omega_{\rm B}}$. Although not visible in Figure 1(a), the bands become progressively narrower as $N_{\rm F}$ increases. Indeed, beyond some critical fermion number $N_{\rm F}^{\rm crit}$ we cannot detect further solutions. This marks an important difference between the approximated analytic predictions of Eqs. (10)-(12) and the full variational solutions. For example, for trap frequencies $\omega_{\rm B}/2\pi = 10, 100$ and 1000, $N_{\rm F}^{\rm crit} \approx 760, 660$ and 620, respectively.

Within the soliton bands, the soliton radial size l_r^0 remains close to $l_{\rm ho}$ throughout. The axial size l_z^0 is infinite at its dispersive boundary and reduces as $a_{{\rm BF}s}$ is made more attractive, with the soliton becoming almost spherical at the point of collapse. This is qualitatively similar to the case for BEC bright solitons [10].

Figure 2 shows how the soliton bands change for differ-

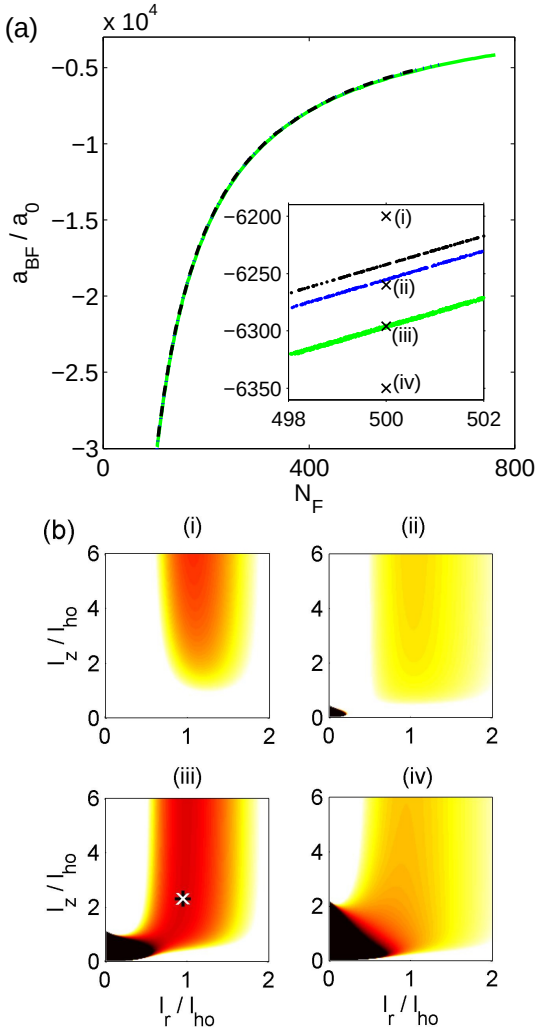

FIG. 1: (a) The bands of soliton solutions in $a_{\mathrm{BF}s} - N_{\mathrm{F}}$ space for a ^{87}Rb-^{40}K mixture with zero p-wave interaction. We present a fixed number of bosons $N_{\mathrm{B}} = 10^5$ and various trap frequencies $\omega_{\mathrm{B}}/2\pi$ =10 (green solid), 100 (blue dotted), 1000 (black dashed) Hz. The inset provides a close up of the soliton bands. (b) Energy landscapes ($\omega_{\mathrm{B}}/2\pi$ = 10Hz, $N_{\mathrm{F}} = 500$ and $N_{\mathrm{B}} = 10^5$) showing four distinct regimes: (i) well above the soliton band ($a_{\mathrm{BF}s} = -6200a_0$), (ii) just above the band ($a_{\mathrm{BF}s} = -6260a_0$), (iii) within the band ($a_{\mathrm{BF}s} = -6296a_0$) and (iv) below the band. ($a_{\mathrm{BF}s} = -6350a_0$). These plots corresponds to the crosses in (a). In (iii) the soliton solution is highlighted by the white cross.

ent number of bosons (in both linear (a) and logarithmic plots (b)). For increasing N_{B} the bands shift to more negative $a_{\mathrm{BF}s}$ and larger N_{F}, and the bands becomes wider as N_{B} is reduced.

Our numerical results predict that, for the numbers of bosons and fermions permitted by our model ($\gg 1$), soliton solutions do not occur at the native Bose-Fermi scattering length $a_{\mathrm{BF}s} = -215a_0$. The soliton solutions exist only for scattering lengths $a_{\mathrm{BF}s} \ll -215a_0$. However, our results show that as N_{B}, and by association N_{F} (since the ratio $N_{\mathrm{B}}/N_{\mathrm{F}}$ must remain within narrow bounds for soliton-supporting conditions to be met, see, e.g., Eqs. (10)-(12)) is decreased the soliton solutions extend to smaller $|a_{\mathrm{BF}s}|$. Indeed, if one were to extrapolate our predictions (beyond its strict regime of validity) to lower atom number, one could imagine that the soliton bands would reach $a_{\mathrm{BF}s} = -215a_0$. Indeed, using a model valid for low atom numbers, Karpiuk *et al.* [18] predict the existence of BF solitons at the native $a_{\mathrm{BF}s} = -215a_0$ for very low atom numbers.

2. *Energy landscape regimes*

To gain physical insight into the system, in Fig. 1(b)(i)-(iv) we present energy landscapes of four distinct regimes in this parameter space. While we present the landscapes for a specific set of parameters ($\omega_{\mathrm{B}}/2\pi = 10$ Hz, $N_{\mathrm{F}} = 500$ and $N_{\mathrm{B}} = 10^5$) the qualitative behaviour is generic. The location of each case is indicated in the inset of Fig. 1(a) by crosses. These four regimes [Fig. 1(i)-(iv)] are as follows:

- (i) Sufficiently above the soliton band, the net contact interactions are repulsive (positive) and the energy landscape consists of a downward 'chute' aligned along the l_z axis. Any wavepacket subjected to this system will disperse axially.

- (ii) Just above the soliton band the net interactions become attractive (negative) and compete with the positive energy terms. The chute remains but the global energy minimum is now at the origin, where the energy diverges to $-\infty$. The attraction is insufficiently strong to support a soliton.

- (iii) Within the band, the play-off between the interspecies attraction and repulsive zero-point kinetic energy leads to a local energy minimum at $[l_r^0, l_z^0]$ (highlighted by the white cross), corresponding to the self-trapped soliton solution.

- (iv) Below the soliton band the attractive interactions dominate the kinetic energy such that the only energy minimum is the global minimum at the origin, representing the collapse instability of the system.

3. *Comparison to the simplified limit of Eqs. (10) and (11)*

In Fig. 2(b) we present a comparison between the variational predictions for the soliton bands and the simplified analytic estimates provided by Eqs. (10) (dashed line) and (11) (dotted line). For ease of observing the differences between the two methods, the data is presented on a log-log plot. For low number of bosons ($N_B = 500$) the variational solutions deviate from the predictions. However, for larger boson number the agreement is excellent. This is to be expected since these predictions assume

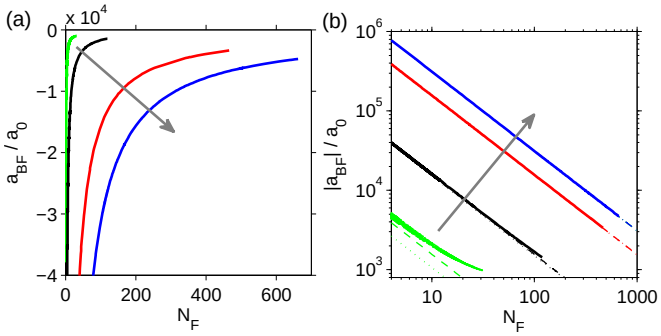

FIG. 2: (a) The bands of soliton solutions in $a_{\mathrm{BF}s} - N_{\mathrm{F}}$ space for no p-wave contributions. We consider fixed trapping $\omega_{\mathrm{B}}/2\pi = 100$Hz and various boson numbers of $N_{\mathrm{B}} = 500$ (green), 5,000 (black), 50,000 (red) and 100,000 (blue). (b) Log-log plot of the soliton bands in (a), with the analytic predictions of Eqs. (10) (dashed line) and (11) (dotted line). The grey arrows indicate the direction of increasing N_{B}.

$N_{\mathrm{B}}/N_{\mathrm{F}} \gg 1$. Indeed for $N_B = 5,000$ and above, the simplified forms give very good predictions for the regimes of soliton solutions (indistinguishable from the full variational results on the scale of this figure).

An important difference, however, is that according to the analytical result, the width of the soliton band decreases as $1/N_{\mathrm{F}}$, becoming vanishingly small only as $N_{\mathrm{F}} \to \infty$. In contrast, the full variational solutions disappear beyond a finite N_{F}. Furthermore, numerically, the bands increase in width as N_{B} is increased, whereas the analytical prediction for the band width is independent of N_{B}.

B. The role of p-wave fermion interactions

1. *Soliton bands in $a_{\mathrm{F}} - N_{\mathrm{F}}$ space*

We now consider the presence of fermion-fermion (p-wave) interactions. We fix the boson-fermion s-wave interaction to its natural value $a_{\mathrm{BF}s} = -215a_0$ and explore the parameter space of $a_{\mathrm{F}} - N_{\mathrm{F}}$. The results are shown in Fig. 3 for fixed boson number $N_{\mathrm{B}} = 10^5$ and various trap frequencies [$\omega_{\mathrm{B}}/2\pi = 10$ (horizontal thatch), 100 (vertical thatch) and 1000 Hz (grey region)]. Recall that in the absence of p-wave interactions, no solitons were obtained for $a_{\mathrm{BF}s} = -215a_0$. In contrast, in the presence of repulsive p-wave fermion-fermion interactions, we now see extensive regions of soliton solutions. The regions become larger for increased trap frequency. This change in size occurs due to a shift in the lower boundary of the regions; the upper boundary is insensitive to ω_{B}, as can be seen in Fig. 3(a).

This enhanced stability when p-wave fermion-fermion interactions are included arises from the fact that the fermion-fermion interaction term in Eq. (5) scales as l^{-5}. Thus, if $a_{\mathrm{F}} > 0$, this term ensures that the energy diverges to positive values as $l \to 0$ and completely

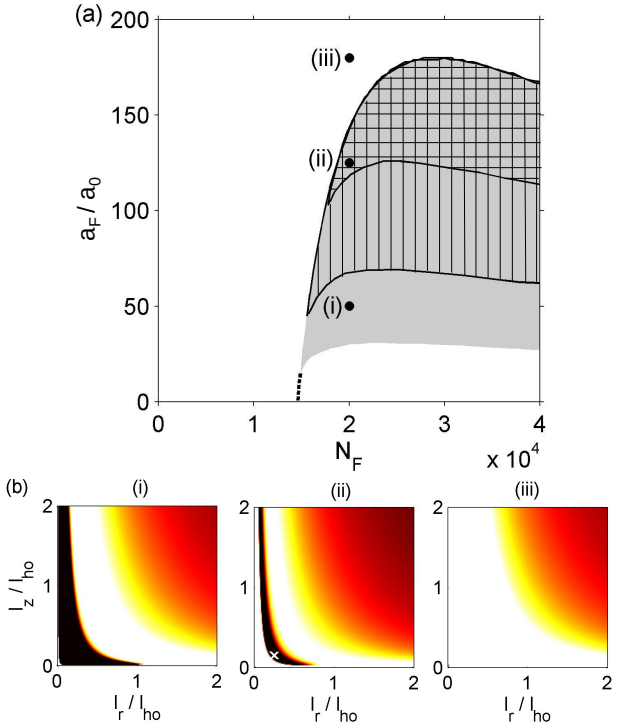

FIG. 3: (a) Soliton bands in $a_{\mathrm{F}} - N_F$ space for boson-fermion interaction $a_{\mathrm{BF}s} = -215a_0$ in presence of fermion-fermion p-wave interactions. The number of bosons is fixed to $N_{\mathrm{B}} = 100,000$ and we present trap frequencies of $\omega_{\mathrm{B}}/2\pi = 10$ (horizontal thatch), 100 (vertical thatch) and 1,000 Hz (grey region). (b) Energy landscapes (for $\omega_{\mathrm{B}}/2\pi = 100$ and $N_{\mathrm{F}} = 20,000$) of (i) below the band ($a_{\mathrm{F}} = 50a_0$) (ii) within the band ($a_{\mathrm{F}} = 125a_0$) and (iii) above the band ($a_{\mathrm{F}} = 180a_0$). The locations of these cases are indicated in plot (a).

removes the presence of a collapse instability. This energetic behaviour is demonstrated by the landscapes shown in Fig. 3(b).

- (i) Below the relevant soliton band (e.g. the band shaded with vertical hatch in Fig. 3(a)) a significant collapse region is present and dominates the energy landscape. However, a positive region is just visible close to the origin in Fig. 3(b)(i).
- (ii) Solutions become supported when the fermion-fermion interaction becomes larger and the play-off between all of the energy contributions generates a local minimum in the energy landscape (white cross).
- (iii) Above the soliton band, the repulsive fermion-fermion interaction becomes so large that it makes the system fully dispersive.

Case (ii) is an intriguing prediction. It suggests that the presence of repulsive p-wave fermion interactions leads to solitons which are the *global* energy minimum of the system. This indicates that such solitons would be far more robust and stable than their bosonic counterparts, which are well-known to exist as meta-stable states prone to an irremovable collapse instability.

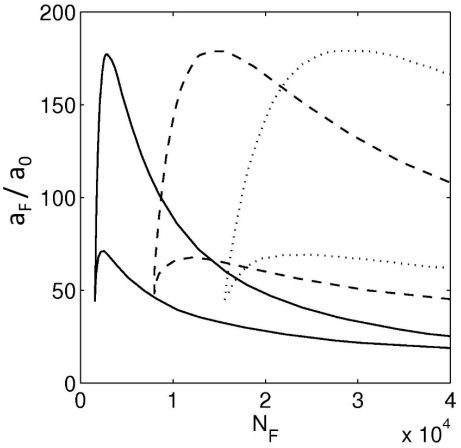

FIG. 4: Soliton bands in $a_{\rm F} - N_F$ space for fixed trap frequency $\omega_{\rm B}/2\pi = 100$ Hz and boson numbers of $N_{\rm B} = 10,000$ (solid), $50,000$ (dashed) and $100,000$ (dotted).

In Fig. 4 we show how the bands change with the number of bosons. As the number of bosons decreases, the bands shift to lower $N_{\rm F}$ and become narrower. Indeed, the bands scale approximately as $1/N_{\rm B}$, i.e. if we plot $N_{\rm F}/N_{\rm B}$ on the x-axis, the bands approximately overlap with each other.

C. Soliton bands in $a_{\rm F} - a_{{\rm BF}s}$ space

The simultaneous manipulation of more than one scattering length has not been experimentally demonstrated. However, in principle, this could be possible through a combination of magnetic, optical and confinement resonances. With this is mind and by way of exploring the soliton solutions further, we now turn to examine the regions of soliton solutions in $a_{\rm F} - a_{{\rm BF}s}$ space [Fig. 5(a)], for fixed $N_{\rm B}$ and $N_{\rm F}$. We will see that parameter space is particularly interesting because it offers the possibility of forming bright soliton solutions as clear *global* minima. In this case, we observe complex-shaped regions of soliton solutions. This includes a large cusp shaped region in the $a_{\rm F} > 0$ half plane. Although not shown, this region extends to indefinitely negative $a_{{\rm BF}s}$. Furthermore, the soliton region features narrow 'fingers' which extend far into the $a_{\rm F} < 0$ half-plane.

We discriminate six distinct regions in this parameter space which we interpret by reference to their typical energy landscapes presented in Fig. 5(b):

- (i) Above this narrow band the landscape is dominated by dispersion with a localised collapse region, but no local minimum exists.

- (ii) Within the soliton band there exists a shallow energy minimum (case(ii)) adjacent to the collapse and dispersive regions.

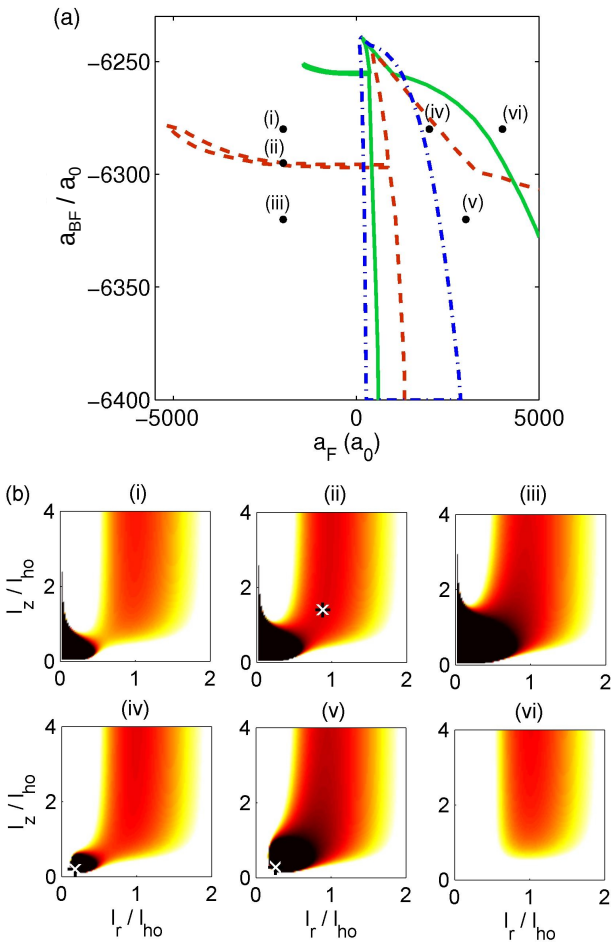

FIG. 5: Soliton bands (as shown by their boundary lines) in the parameter space of $a_{\rm F}$ and $a_{{\rm BF}s}$. (a) We fix $N_{\rm B} = 100,000$ and $N_{\rm F} = 500$, and use $\omega_{\rm B}/2\pi = 10$ (red dashed), 100 (green solid) and $1,000$ (blue dot-dashed) Hz. (b) Energy landscapes for the $\omega_{\rm B}/2\pi = 10$ case at the points (i) $a_{\rm F} = -2000a_0$, $a_{{\rm BF}s} = -6280a_0$, (ii) $a_{\rm F} = -2000a_0$, $a_{{\rm BF}s} = -6295a_0$, (iii) $a_{\rm F} = -2000a_0$, $a_{{\rm BF}s} = -6320a_0$, (iv) $a_{\rm F} = 2000a_0$, $a_{{\rm BF}s} = -6280a_0$, (v) $a_{\rm F} = 3000a_0$, $a_{{\rm BF}s} = -6320a_0$, and (iv) $a_{\rm F} = 4000a_0$, $a_{{\rm BF}s} = -6280a_0$. These points are denoted in (a).

- (iii) Below the soliton band the whole landscape is unstable to collapse.

- (iv, v) In the regions containing points (iv) and (v) there is no collapse region at the origin and there exists a well-localised and deep energy minimum denoting a soliton solution.

- (vi) This region is dispersive due to the dominance of repulsive interactions.

Regions (i),(ii),(iii) and (vi) possess energy landscapes which are analogous to those seen in Fig. 1(b). However, the most intriguing regions are (iv) and (v). These solutions are the most common type that exist in this parameter space. Like the observation in Fig. 3(b)(ii), the soliton now becomes the *global* energy minimum of

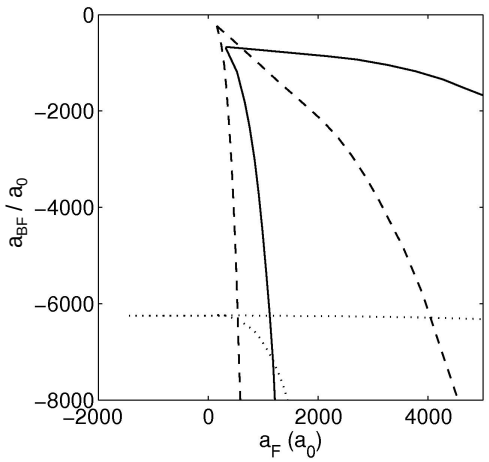

FIG. 6: Soliton bands in the parameter space $a_{\rm F} - a_{{\rm BF}s}$ (shown by their boundary lines). We fix $\omega_{\rm B}/2\pi = 100$Hz and $N_{\rm F} = 500$ and consider $N_{\rm B} = 1,000$ (dashed line), $10,000$ (solid line) and $100,000$ (dotted line).

the system. However, these landscapes are strikingly well localised and deep. The depth of this minimum is typically of the order of $100\hbar\omega_{\rm B}$. For comparison, for a bright bosonic soliton the depth of the energy minima is of the order of $0.1\hbar\omega_{\rm B}$. Within the context of our scaling solutions (fixed gaussian shape), this depth and narrowness of the energy minima indicates extreme stability of the solutions to shape modification, including collapse and dispersion.

For completenesss, Fig. 6 demonstrates how these extensive soliton regions in $a_{\rm F} - a_{{\rm BF}s}$ space become modified for different N_B. The presence of the "fingers" is sensitive to $N_{\rm B}$ but the main region of solutions persists, albeit shifting to more negative $a_{{\rm BF}s}$ with increasing $N_{\rm B}$.

While here we have limited our study to the p-wave interactions of only the fermions, the same qualitative soliton regimes and solutions are obtained if the p-wave boson-fermion interaction is included instead (or, indeed, if both are included). This is because the p-wave fermion-boson interaction has the same functional form (scaling as l^{-5}).

IV. DISCUSSION AND CONCLUSION

Our results show that in the absence of p-wave contributions the range of soliton solutions is rather limited, being confined to narrow bands in $a_{\rm BF} - N_{\rm F}$ space. Indeed, the solutions behave similarly to bright bosonic solitons but with an effective scattering length. While reducing the radial confinement widens the soliton bands, this also makes the system more prone to collective excitations which may disrupt the soliton. For a ^{87}Rb-^{40}K mixture and in the validity regime of our approach ($N_{\rm B}, N_{\rm F} \gg 1$) we cannot locate soliton solutions at the native boson-fermion scattering length of $-215a_0$. Values of around $-1000a_0$ are required to reach a soliton band at these atom numbers. The work of Karpiuk *et al.* demonstrated that atom numbers of order unity are required to support Bose-Fermi solitons at the native ^{87}Rb-^{40}K scattering length. While the scattering length can be engineered to large values through scattering resonance tuning, the ensuing soliton bands are so narrow that experimentally locating them is likely to be problematic. Furthermore, there remains a collapse instability in the system and the ratio of bosons to fermions is constrained to small values. In contrast, the presence of repulsive p-wave fermion-fermion interactions has a dramatic stabilizing effect on the system. This can lead to a removal of the collapse instability such that the soliton solutions become *global* energy minima. We find extensive soliton regimes, in which the soliton minima are extremely deep, suggesting that they may form soliton structures that are considerably more robust than in the absence of p-wave interactions. The p-wave interaction also provides a strong tuning parameter, enabling the boson-fermion ratio to be dramatically varied. Importantly, for a potential experimental realization of BF solitons, we find extensive soliton solutions at the native boson-fermion interaction and with only moderate fermionic interactions.

The remarkable capacity of repulsive p-wave interactions to remove the collapse instability stems from the scaling behaviour of its energy contribution. Denoting a generalized lengthscale of the gaussian wavepacket as ℓ, the total variational energy of the Bose-Fermi system is of the form,

$$E \sim \frac{1}{\ell^2} + \ell^2 \pm \frac{1}{\ell^3} \pm \frac{1}{\ell^5}. \qquad (13)$$

The first two terms, the kinetic and potential energy terms, are always positive. The last two terms, the s-wave and p-wave interaction energies, respectively, may be positive or negative. In the absence of p-wave interactions, a negative s-wave term will cause the energy to diverge to $-\infty$ as $\ell \to 0$, signifying the presence of the collapse instability. For non-zero p-wave interactions, the p-wave term dictates the fate of the system as $\ell \to 0$ and importantly, for positive p-wave interactions the collapse divergence is completely removed.

It is important to note that this scaling behaviour originates from the Thomas-Fermi approximation and so is not limited to gaussian wavepackets. Consider homogeneous Bose and Fermi gases in a large hard-wall box of volume ℓ^3. It is trivial to see from Eqs. (2) and (4) that the energy scales as above, minus the ℓ^2 term. Thus it is clear that the capacity of repulsive p-wave interactions to stabilise against collapse is likely to extend to trapped Bose-Fermi mixtures in general.

While we have presented results for p-wave interactions in only the fermion-fermion case, we find qualitatively similar soliton regions, landscapes and conclusions when including boson-fermion p-wave interactions instead. This is because the same energy scaling discussed above applies.

In conclusion, according to a variational model, the presence of repulsive p-wave interactions in Bose-Fermi mixtures removes the usual collapse instability and leads to stable, robust bright soliton solutions that are global energy minima of the system. We have discussed specifically the boson-fermion pairing of ^{87}Rb and ^{40}K, but the stabilizing effect of repulsive p-wave interactions should apply in general to other ultracold Bose-Fermi mixtures. Given that the collapse instability has proved a major hindrance to the controlled generation, manipulation and interaction of matter-wave solitons to date, these more stable p-wave entities may provide a more versatile route to explore and exploit the special characteristics of solitons.

[1] J Scott Russell, in Report on Waves, Proceedings of the Meeting of the British Association for the Advancement of Science, York (London 1845)

[2] A.A.Levchenko et al., JETP Lett. **65**, 573 (1997)

[3] G. I. Stegeman and M. Segev, Science **286**, 1518 (1999)

[4] L. Khaykovich et al., Science **296**, 1290 (2002)

[5] K. E. Strecker et al., Nature 417 **150**, (2002)

[6] S. L. Cornish et al., Phys. Rev. Lett. **96**, 170401 (2006)

[7] N. G. Parker, A. M. Martin, S. L. Cornish and C. S. Adams, J. Phys. B **41**, 045303 (2008)

[8] T. P. Billam, S. L. Cornish, S. A. Gardiner, Phys. Rev. A **83**, 041602(R) (2011)

[9] S. L. Cornish, N. G. Parker, A. M. Martin, T. Judd, M. Fromhold and C. S. Adams, Physica D **238**, 1299 (2009)

[10] V. M. Perez-Garcia, H. Michinel and H. Herrero, Phys. Rev. A **57**, 3837 (1998); N. G. Parker , S. L. Cornish, C. S. Adams, and A. M. Martin, J. Phys. B **40**, 3127 (2007); N. G. Parker, A. M. Martin, C. S. Adams and S. L. Cornish, Physica D **238**, 1456 (2009).

[11] L. D. Carr and Y. Castin, Phys. Rev. A **66**, 063602 (2002).

[12] A. G. Truscott *et al.*, Science **291**, 2570 (2001); F. Schreck *et al.*, Phys. Rev. Lett. **87**, 080403 (2001).

[13] Z. Hadzibabic *et al.*, Phys. Rev. Lett. **88**, 160401 (2002).

[14] G. Roati *et al.*, Phys. Rev. Lett. **89**, 150403 (2002); S. Inouye, J. Goldwin, M.L. Olsen, C. Ticknor, J.L. Bohn, D.S. Jin, Phys. Rev. Lett. **93**, 183201 (2004); C. Ospelkaus, S. Ospelkaus, K. Sengstock and K. Bongs, Phys. Rev. Lett. **96**, 020401 (2006); C. Klempt *et al.*, Eur. Phys. J. D **48**, 121 (2008).

[15] G. Modugno, G. Roati, F. Riboli, F. Ferlaino, R. J. Brecha and M. Inguscio, Science **297**, 2240 (2002).

[16] T. Fukuhara, S. Sugawa, Y. Takasu and Y. Takahashi, Phys. Rev. A **79**, 021601 (2009).

[17] M. K. Tey, S. Stellmer, R. Grimm and F. Schreck, Phys. Rev. A **82**, 011608 (2010).

[18] T. Karpiuk et al., Phys. Rev. Lett. **93**, 100401 (2004); T. Karpiuk et al., Phys. Rev. A **73**, 053602 (2006).

[19] S. K. Adhikari, Phys. Rev. A **72**, 053608 (2005); J. Santhanam et al., Phys. Rev. A **73**, 013612 (2006); L. Salasnich et al., Phys. Rev. A **75**, 023616 (2007)

[20] P. A. Ruprecht, M. J. Holland, K. Burnett and M. Edwards, Phys. Rev. A **51**, 4704 (1995); J. L. Roberts, N. R. Claussen, S. L. Cornish, E. A. Donley, E. A. Cornell and C. E. Wieman, Phys. Rev. Lett. **86**, 4211 (2001); A. Gammal, T. Frederico and L. Tomio, Phys. Rev. A **64**, 055602 (2001).

[21] C. J. Pethick and H. Smith, *Bose-Einstein Condensation in Dilute Gases* (Cambridge University Press, 2001).

[22] K. Molmer, Phys. Rev. Lett. **80**, 1804 (1998); A. M. Belemuk, V. N. Ryzhov and S. T. Chui, Phys. Rev. A **76**, 013609 (2007); S. Röthel and A. Pelster, Eur. Phys. J. B **59**, 343 (2007).

[23] R. Roth and H. Feldmeier, Phys. Rev. A **64**, 043603 (2001); R. Roth and H. Feldmeier, Phys. Rev. A **65**, 021603(R) (2002); R. Roth, Phys. Rev. A **66**, 013614 (2002).

[24] T. Karpiuk, M. Brewczyk, M. Gajda and K. Rzazewski, J. Phys. B **38**, L215 (2005).

[25] X. J. Liu, M. Modugno and H. Hu, Phys. Rev. A **68**, 053605 (2003).

[26] H. Saito and M. Ueda, Phys. Rev. Lett. **90**, 040403 (2003); F. K. Abdullaev, J. G. Caputo, R. A. Kraenkel, and B. A. Malomed, Phys. Rev. A **67**, 013605 (2003); S. K. Adhikari, ibid. **69**, 063613 (2004); G. D. Montesinos, V. M. Perez-Garcia, and P. J. Torres, Physica D **191**, 193 (2004); V. V. Konotop and P. Pacciani, Phys. Rev. Lett. **94**, 240405 (2005); A. Itin, T. Morishita, and S. Watanabe, Phys. Rev. A **74**, 033613 (2006).

[27] F. Dalfovo and S. Stringari, Phys. Rev. A **53**, 2477 (1996); S. K. Adhikari, Phys. Rev. E **65**, 016703 (2001); S. K. Adhikari, Phys. Rev. A **66**, 043601 (2002); S. K. Adhikari, New J. Phys. **5**, 137 (2003); N. A. Jamaludin, N. G. Parker and A. M. Martin, Phys. Rev. A **77**, 051603(R) (2008); N. A. Jamaludin, Phys. Rev. A **83**, 059910(E) (2011); M. C. Tsatsos, A. I. Streltsov, O. E. Alon and L. S. Cederbaum, Phys. Rev. A **82**, 033613 (2010); J. Abdullaev, A. S. Desyatnikov and E. A. Ostrovskaya, J. Opt. **13**, 064023 (2011).

[28] L. S. Cederbaum, A. I. Streltsov and O. E. Alon, Phys. Rev. Lett. **100**, 040402 (2008).

[29] C. A. Regal, C. Ticknor, J. L. Bohn and D. S. Jin, Phys. Rev. Lett. **90**, 053201 (2003); J. Zhang *et al.*, Phys. Rev. A **70**, 030702(R) (2004); K. Günter, T. Stöferle, H. Moritz, M. Köhl and T. Esslinger, Phys. Rev. Lett. **95** 230401 (2005); Y. Inada *et al.*, Phys. Rev. Lett. **101**, 100401 (2008); J. Fuchs *et al.*, Phys. Rev. A **77**, 053616 (2008).

[30] P. Massignan, A. Sanpera and M. Lewenstein, Phys. Rev. A **81**, 031607(R) (2010).

[31] F. Ferlaino *et al.*, Phys. Rev. A **73**, 040702(R) (2006); Phys. Rev. A **74**, 039903(E) (2006).

[32] K. K. Das, Phys. Rev. Lett. **90**, 170403 (2003).

[33] N. Nygaard and K. Molmer, Phys. Rev. A **59**, 2974 (1999)

[34] E. G. M. van Kempen, S. J. J. M. F. Kokkelmans, D. J. Heinzen and B. J. Verhaar, Phys. Rev. Lett. **88**, 093201 (2002).